Eurasian Journal of Soil Science 2024, 13(3), 210 - 223

Eurasian Journal of Soil Science

Journal homepage : http://ejss.fesss.org

Nomograph development for water erosion quantification in Wadi Cheliff's catchment, Northern Algeria

Ilhem Bouaichi *, Bénina Touaibia

Mobilization and Valorization of Water Resources Laboratory (MVRE), National Higher School for Hydraulics (ENSH), Soumaa road 29, Blida, Algeria

Article Info

Received : 18.09.2023
Accepted : 15.03.2024
Available online: 19.03.2024

Author(s)

I.Bouaichi *
B.Touaibia

* Corresponding author

Abstract

Water erosion study is regarded as one of the most important axes in scientific researches. The erosive effect of water on the surface layers can have major consequences on soil loss and land degradation. The objective of our work was the development of a water erosion nomograph that represents a practical and precise tool that is adapted to local conditions for a direct quantification of erosive action in the absence of basic data. Regarding the magnitude of the phenomenon in Algeria, the catchment of Wadi Cheliff was taken as an experimental site where a significant spatio-temporal variability of liquid and solid flows was observed and the measurement network in different locations was either dispersed or non-existent. The developed methodological approach permitted the identification of 149 experimental sites (20 hydrometric stations, 15 large dams and 114 hill dams) where existing data allowed the erosion quantification. A flow coefficient variography was performed in addition to a principal component analysis (PCA), leading to the identification of three distinct groups. Moreover, the modeling of the studied variable was achieved through the application of multivariate analysis to the third group of 100 observations. Applying the principles of nomography on the final model, a nomograph of the semi-arid area of Wadi Cheliff catchment was realized for surfaces ranging from 500 to 25 000 ha. This nomograph enabled the direct quantification of water erosion from the product ($Es_1 \times Es_2$), taking into account the area of the catchment, its average slope and its flow coefficient with a mean absolute percentage error (MAPE) of 2%.

Keywords: Multivariate analysis, nomograph, PCA, variography, Wadi Cheliff, water erosion.

Introduction

The frequent presence of excessive suspended sediment in streams is a relevant indicator of water erosion problems within a catchment. In order to assess the extent of these problems and understand their consequences, it is crucial to measure the sedimentation rates reaching the outlet. From the perspective of sustainable management and preservation of natural water and soil resources at the catchment, it becomes essential to quantify water erosion accurately, which allows the identification of areas likely to produce high levels of sediment.

In North Africa, erosive action is a significant threat. The majority of catchments in Algeria, Tunisia and Morocco are characterized by a strong degradation, exceeding 20 T ha^{-1} per year (Remini and Remini, 2003).

The erosion rate quantification is a complex and challenging task in practice due to the various factors contributing to its increase (Megnounif et al., 2007; Ochoa et al., 2016; Dengiz and Demirkaya, 2022; Najafova, 2022). This task becomes particularly difficult in practice especially when watersheds are not gauged with the absence of a well-established monitoring network that provides the basic data, so it gets challenging to measure spatial-temporal variability of erosion processes. Without these data, it is also difficult to establish references for comparing changes over time. Indeed, the lack of these essential elements significantly complicates the direct quantification; thus, the use of other methods is essential for a precise measurement of

: https://doi.org/10.18393/ejss.xxxxxxx
: http://ejss.fesss.org/10.18393/ejss.xxxxxx
Publisher : Federation of Eurasian Soil Science Societies
e-ISSN : 2147-4249

the water erosive action on the soil. Among the most widely used methods today, Digital Terrain Model and Geographic Information System, remote sensing space, models based on physical processes of soil particle detachment, geophysical techniques and hydrological models. Various erosion modelling studies, including Touaibia et al. (2001), López-Tarazón et al. (2010), Eisazadeh et al. (2012), Meddi et al. (2014) and Heng and Suestugi (2015), have contributed to the understanding of the erosive process rate, despite the absence of data.

Nowadays, although numerical and computational methods have become predominant in hydrology, nomography remains an interesting technique for understanding the relationships between different variables and performing rapid calculations. The earliest nomographs originated in the late 19th and early 20th centuries, and they are still very useful. However, the advent of nomographic science and its use on hydrological modeling remains poorly employed today. In the 1840s, there was an emergence of articles discussing the effect of deformation on graphic representations known as nomographs, in order to enhance their readability. Over the following decades, documents on analytical criteria for graphical representation were produced. The initial documentation by d'Ocagne in 1884, detailing various types of nomographs, serves as a reference point, as mentioned by Jahnke (2012).

When performing intricate numerical calculations, it is beneficial to utilize a nomograph. This graphic representation is depicted through lines or fixed points with appropriately marked scales, whether mobile or not. According to Tournès (2000), a simple reading provides the intended value based on the parameters. Additionally, their adaptability and flexibility to a wide range of situations support their utilization (Tran Van, 1961). Thus, nomographs or abacus represent graphic tables playing the same role as numerical tables. They are often based on empirical equations that were developed from field observations and experimental data.

In this context, the objective of our work was the application of nomography which represents a discipline less frequently used nowadays, and its association with new computational methods such as numerical modeling, variograph and statistical methods for quantifying the complex phenomenon of water erosion of a watershed. Indeed, only the nomograph of Wischmeier and Smith developed in 1960 and updated in 1978, provides a graphical representation of the universal soil loss equation that allows users to directly read the estimated values of the various parameters of the equation for the quantification of the erosive rate.

The Wadi Cheliff catchment is considered as a study area given its large territory and the weakness of its measurement network. With the absence of hydrometric stations and their concentration in the north of the basin, it is crucial to identify every structure that is susceptible to silting. Hence, 149 sites were listed with 20 hydrometric stations measuring liquid and solid flows, as well as 15 large dams and 114 hill dams contributing to the calculation of the erosion rate from their siltation rate. This identification permitted the establishment of a particular methodology for the development of an erosion nomograph that links it to the basin's flow coefficient as well as its morphometric coefficients (slope and surface). The methodology that was adopted included the following:

- Identification of 149 experimental sites throughout the basin,
- Quantification of specific erosion at site watershed level,
- Determination of the different influencing factors, namely the surface area of each site, its drainage density, its average slope, its vegetation cover and its flow coefficient. This last parameter was variographed,
- PCA application for the identification of homogeneous areas,
- Search for a regressive model via multivariate analysis,
- Trace and validate the nomograph using a programming algorithm.

Material and Methods

Presentation of the study area

The Wadi Cheliff's catchment, with its main stream extending 759 km and draining an area of 4 375 000 ha at its mouth, is an important Wadi in North Africa due to its annual water supply. It plays a major role in the hydrographic system of Algeria since it is the only river that drains part of the highlands to cross the Cheliff valley and join at its outlet the Mediterranean Sea near Mostaganem. It owes its character to the deep structure of the landscapes it crosses.

The study area extends between longitudes 0° 7' and 3° 31' East and between latitudes 33° 53' and 36° 26' North. It is bordered to the North by the coastal catchments of Algiers and Oran, to the East by the catchments of Isser, Hodna, Zahrez, and the high plateaus of Constantine, to the West by the basins of Macta and the high

plateaus of Oran, in addition to the Saharan Atlas to the South (Figure 1a). It is divided into two distinct regions:

- The upstream part of the Cheliff with an area of 2 050 000 ha, limited to the south by the mountains of Jebel Amour and to the north by the Ouarsenis mountains;
- The downstream part of the Cheliff, which covers an area of 2 325 000 ha, bounded to the south by the mountain ranges of Tiaret, Saida and Ouarsenis, and by the Dahra and Beni Menacer to the north.

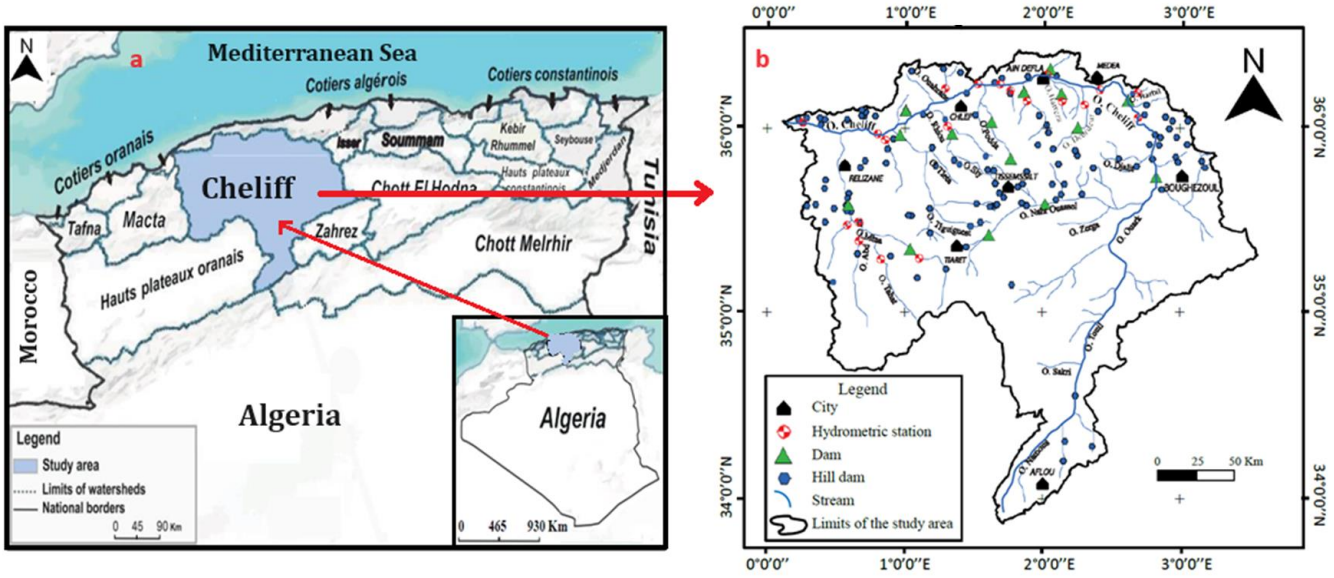

Figure 1. Catchment of Wadi Cheliff and its network measures
(a: Location of the study area; b: Location of experimental sites in the study area)

Its altitudes range from 0 to 1983 m. Almost all of its soils are alluvial, consisting mainly of fine components derived from marls or clays, making soils more vulnerable to erosion (Bouchelkia and Remini, 2003).

Additionally, its climate is semi-arid Mediterranean characterized by irregular spatio-temporal rainfall patterns. Furthermore, the average annual precipitation is 357 mm, it oscillates between values less than 150 mm in the South and values close to 700 mm in the Northeast sector. While the average annual temperature for the entire basin is estimated at 19.2°C. The surface runoff obviously undergoes the influence of the marine rain regime which is characterized by the succession of a rainy and cold season with considerable floods and a very marked dry and hot summer season with a non-significant flow, thus the average annual runoff varies from 3% to 35% at the outlet of the basin.

Moreover, the measurement network identified for our study includes 149 experimental sites that were distributed homogeneously as follow: 20 hydrometric stations, 15 large dams and 114 hill dams, in order to cover the entire study area (Figure 1b).

Database

The used data for water erosion quantification are gathered from the National Agency of Water Resources for hydrometric stations (13 to 56 years of operation), from the National Agency of Dams and Transfers for dams, and from the Agency of Hydrographic Basin Cheliff-Zahrez for hill dams. They are presented under shape:

For data from hydrometric stations, the files include:

- Instantaneous liquid flows Ql ($m^3\ s^{-1}$).
- Instantaneous concentrations C ($g\ L^{-1}$).
- Instantaneous solid flows Qs ($kg\ s^{-1}$).
- Average daily flows Qad ($m^3\ s^{-1}$).

For dams and hill reservoirs, the files gather:

- Bathymetric surveys of the dams.
- Data of dams releases: date, inputs, total consumption (drinking water supply, irrigation, other), distributaries (leakage, bottom outlet, discharge, desludging and evaporation), available water volume and so the filling rate.
- Identification of hill reservoirs: code, name, structure nature, geographic coordinates (X, Y and Z), Wadi, catchment surface, year into service, initial capacity, destination, actual state and operational duration.

Quantification approach of the specific erosion

At hydrometric station level

Building on the scientific work of Touaibia et al. (2001), Ammari (2012) and Kheniche et al. (2019), our approach is based on homogenisation and data extension via a functional relationship of solid flow – liquid flow. Regressive models requested are of type: linear, logarithmic, power, exponential and polynomial. The monthly-scale scatter diagram identified the power-like regressive pattern as follows:

$$Q_s = a \times Q_l^b \quad (1)$$

With: Qs : solid flow (kg s^{-1}); Ql : liquid flow (m^3 s^{-1}); a , b : coefficients.

The explained variance by determination coefficient is satisfactory. This latter represents 57% to 87% of the total variance.

Relationship (1) allowed quantifying the solid transport Qs in suspension at daily, monthly and annual scales on the whole observation period (Bouchelkia and Remini, 2003; Bouanani, 2004; Lee and Kang, 2014).

For thrust, works of Mokhtari (2005), Larfi and Remini (2006) and Elahcène (2013) estimated it to 19%, 32% and 11% respectively for some similar basins. An average of 20% is retained; it is supported by works of Touaibia (2000) on tributaries of the considered basin (O.Mina).

The release of dams contributed to the erosive phenomenon. On the 20 hydrometric stations, 10 among them are located below the 15 considered dams. These releases contribute from 2% to 70% to the annual sediments inputs, which varies from one station to another according to the dams' number located upstream and their activity state. On average, we estimate that 40% of the annual sediments quantities are transited or deposited only for tributary stations of the dams.

The annual values of the specific erosion (Es) vary considerably passing from 2.64 to 13.91 T ha^{-1}, corresponding to areas of 253 700 ha and 47 000 ha, respectively. The surface effect is to be taken into consideration because its influence is direct on the quantification of Es.

At dam's level

The quantification of Qs (sediment and thrust) was carried out at the level of 15 catchment dams from the latest bathymetric campaigns carried out between 2018 and 2019.

The Boughezoul dam records the lowest annual soil loss, i.e. Es = 0.26 T ha^{-1}, for an estimated annual siltation volume of 0.489 Mm^3 and corresponding to a surface of 1 873 000 ha. Likewise, for the Deurdeur dam, which loses annually a volume of 0.470 Mm^3 of its storage capacity, Es is estimated to 10.05 T ha-1 for a surface of 46 800 ha. This reflects directly the surface effect on quantification of the phenomenon under study.

The dam's watershed of Wadi Fodda presents the maximum annual degradation of soil of about 48.28 T ha^{-1}. This corresponds to an annual silting volume and to a surface estimated, respectively, to 1.738 Mm^3 and 36 000 ha. Otherwise, for the Gargar's dam, which receives in its basin an annual mud volume that is 3 times upper than its previous volume, i.e. 5.717 Mm^3, Es is equal to 23.92 T ha^{-1} for a surface of 239 000 ha. This confirms the surface effect which intervenes once again on the Es values.

At hill dam's level

Hillside reservoirs mobilize surface water structures intended for irrigation. With 114 structures, they make up over 75% of the monitoring network. Their representative spatial distribution of the watershed allowed scanning the whole study area. Knowing capacity storage, surface of their watershed and their expected lifetime, Es is calculated directly (Abdellaoui et al., 2002).

Specific erosion multivariate analysis

Identification of explanatory variables

According to Touaibia and Achite (2003), Zhou et al. (2008), Bouchnak et al. (2009) and Shen et al. (2016), five explanatory variables are selected for multivariate analysis, it is about:

- Surface of the catchment (S ; ha): It has a direct effect and it is inversely proportional to the specific erosion. As for 149 sites, surface varies from 480 ha to 1 873 000 ha, with a variation coefficient (Cv) of 3.55.
- Draining density (Dd ; km km^{-2}): It is the ratio of the length sum of a catchment's water courses on its surface. Its values vary from 0.40 to 1.87 km km^{-2}, with a Cv of 0.36.
- Average slope of the catchment (P ; %): Expressed in %, it allows determination and classification of the relief. Its increase proportionally causes that of water erosion (El Kateb et al., 2013). Slope is determined from the Digital Elevation Model (DEM) with a resolution of 30 m, downloaded from ASTER GDEM. Average values vary from 4.15% to 21.48%.

- Flow coefficient (Cf ; %): It is the ratio between the average death of runoff and the effective rainfall. Used database includes 50 measurements, where Cf is calculated based on hydrometric and rainfall data. Study of variography and its interpolation by Krigeage method have identified the spherical model, for representation of Cf variography (Figure 3c). Its function γ(h) is given by the following formula (2). Values of Cf vary from 2.2% to 35%.

$$\gamma(h) = 54 + 25\left[\frac{3}{2}\left(\frac{h}{41.5}\right) - \frac{1}{2}\left(\frac{h}{41.5}\right)^3\right] \quad (2)$$

- Vegetation cover rate (Cveg ; %):

It is considered as one of the variables playing an important role against water erosion (Rey et al. 2004). Its determination required collection of 12 land use maps of the wilayas covering the study area, obtained from National Institute of Soil, Irrigation and Drainage. These maps were assembled in order to produce the land use map of the Wadi Cheliff's catchment. The resulting map demonstrated that the vegetation cover rate of the 149 sites varies from 1.03% to 88.24%.

On Figure 2, an organizational chart is developed explaining different determination phases of explanatory variables corresponding to different measure sites. The resulting maps are illustrated in Figure 3.

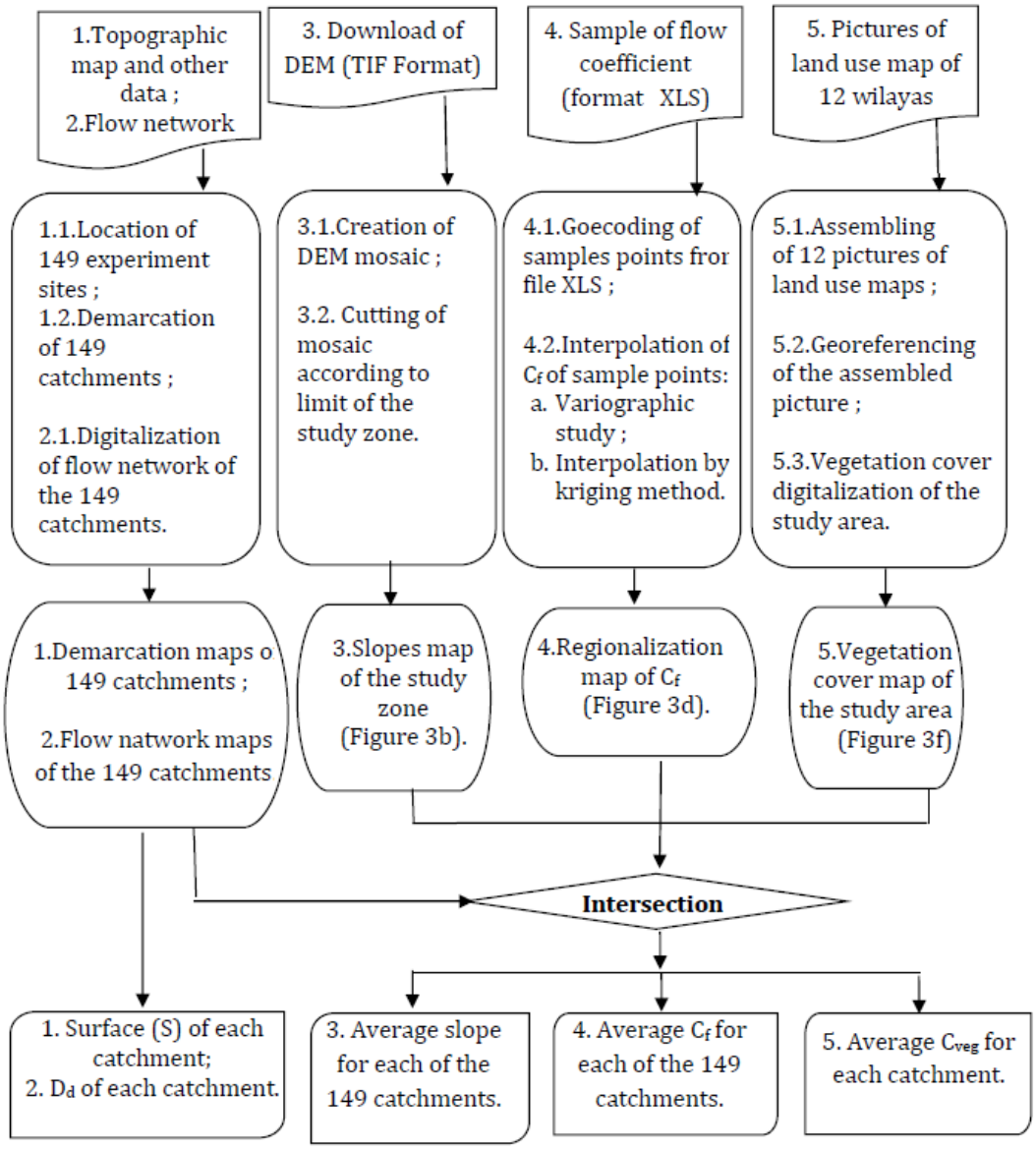

Figure 2. Organizational chart adopted for determination of explanatory variables.

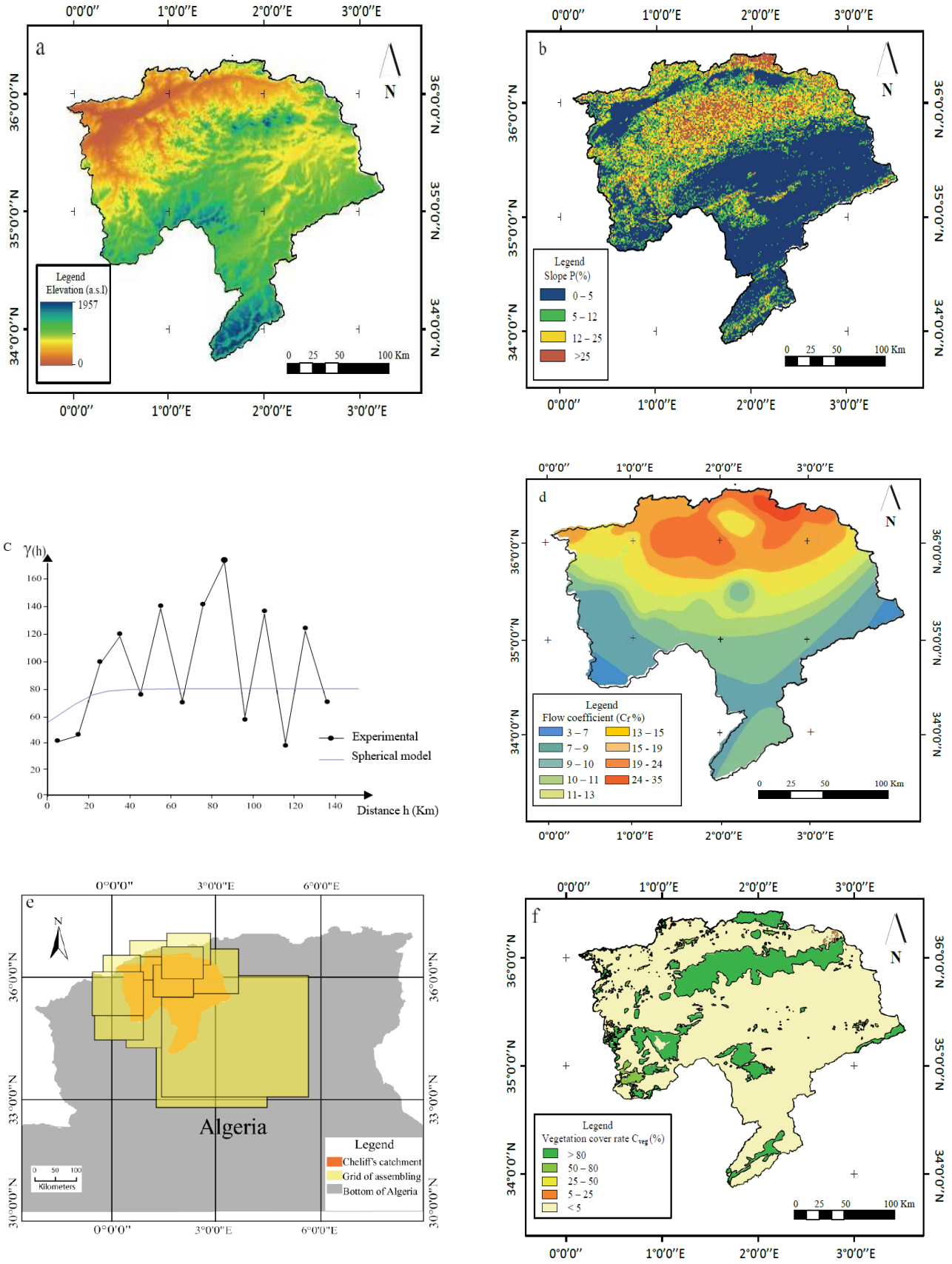

Figure 3. Determination maps of explanatory variables of Wadi Cheliff's catchment
(a: Digital Elevation Model (DEM), b: Slopes map, c: Variogram of flow coefficient, d: Flow coefficient regionalization, e: Basin map for assembly of 12 wilayas, f: Vegetation cover rate)

Principal Components Analysis (PCA)

It is considered as being a very powerful method to explore structure of a high number "P" of quantitative data by observed element (Hotelling, 1933). PCA is applied on a matrix of 149 lines and 6 columns. Two cases are taken into consideration; with and without varimax rotation of orthogonal axes. Correlation matrix (Table 1) shows that between Es and explanatory variables Dd, P and Cf, the relationships are the most significant at the tolerance level of 5% with correlation coefficients estimated respectively at 0.66, 0.70 and 0.73.

Sites assembly allowed identification of the factorial axes responsible of spatial distribution. This underlines heterogeneities between groups and deduces variables that best characterize each group. Percentages of cumulative variances show that the three first components C1, C2 and C3, explaining 85.21% of the total data, are retained. Contributions of projected variables after varimax rotation (Table 1) show dominance of S on axe C3 and of Cveg on axe C2 (Figure 4e) where 37.35% of inertia is cumulated.

Projection of individuals on axes C2-C3 (Figure 4f), makes three distinct groups:

- The first group of 23 individuals is characterized by surfaces relatively large associated to weak values of Es and inversely. It highlights the direct effect of the surface on its qualification according to its magnitude order.
- The second group, where 22 individuals are gathered, is characterized by very dense Cveg rates to which correspond relatively important Es values.
- As for the third group, which gather 104 individuals, it is characterized by a positive proportionality, on the first hand, between Es and variables Dd, P and Cf, and on other hand, negative proportionality between Es and variables S and Cveg. This group avoids influence of the surface and rate of vegetation cover on the specific erosion estimate. It will be subject of a multivariate analysis.

Table 1. Correlation matrix of PCA and variables contribution according to the axes

Variables	Correlation matrix before PCA						Contribution of the variables according to the axes C_1, C_2 and C_3 (%)		
	Es	S	D_d	P	C_f	C_{veg}	C_1	C_2	C_3
Es	1						27.18	4.46	0.32
S	-0.17	1					0.46	0.00	95.85
D_d	0.66	-0.15	1				15.87	18.97	0.26
P	0.70	-0.24	0.41	1			27.63	3.71	2.24
C_f	0.73	-0.21	0.52	0.82	1		28.84	0.02	1.33
C_{veg}	-0.17	-0.01	-0.27	0.13	-0.03	1	0.01	72.83	0.00

Multivariate analysis: application of multiple regressions

1st case: 3rd group (104 values)

Research of a functional relationship between the studied variable and explanatory variables is done by stepwise regression, allowing to eliminate each time the less correlated variation based on correlation coefficient (r) for error P = 5% (Dagnelie, 1992). The non-linearity of the studied relationship duly demonstrated (Borges, 1993; Achite and Meddi, 2005). Its application highlights the matrix of variables correlation (Table 2). The correlation coefficients are clearly improved between Es and variables S and Cveg going from -0.17 to -0.87 and from -0.17 to -0.53, respectively. The resulting regression models show that the regression fit lies between Es and all other variables, with R^2 at its highest value of 0.83 (Table 2). The adjustment of the predicted values by the selected model compared to the measured values presents four observations outside the confidence intervals fixed at 95%. Application of Kolmogorov-Smirnov's test becomes indispensable to make up mind whether these observations are to be taken into account or not.

Results display D statistic test which represents the highest difference between the two cumulated frequency curves of the two samples, and thus the p-value (to be compared to the meaning threshold, *P, generally fixed at 5%). This latter is the probability to have the same values under the hypothesis Ho (null hypothesis that two samples come from the same distribution), otherwise an alternative hypothesis H1 (that these same samples come from distribution having different apportionments). With D = 1 and p-value = 2.86% (which is inferior to *P), the Ho hypothesis is rejected in favour of the alternative H1 hypothesis. Measured values are very different from those predicted. These four comments are to be excluded from the series, with a size of 100 measurements, and the regression restudied.

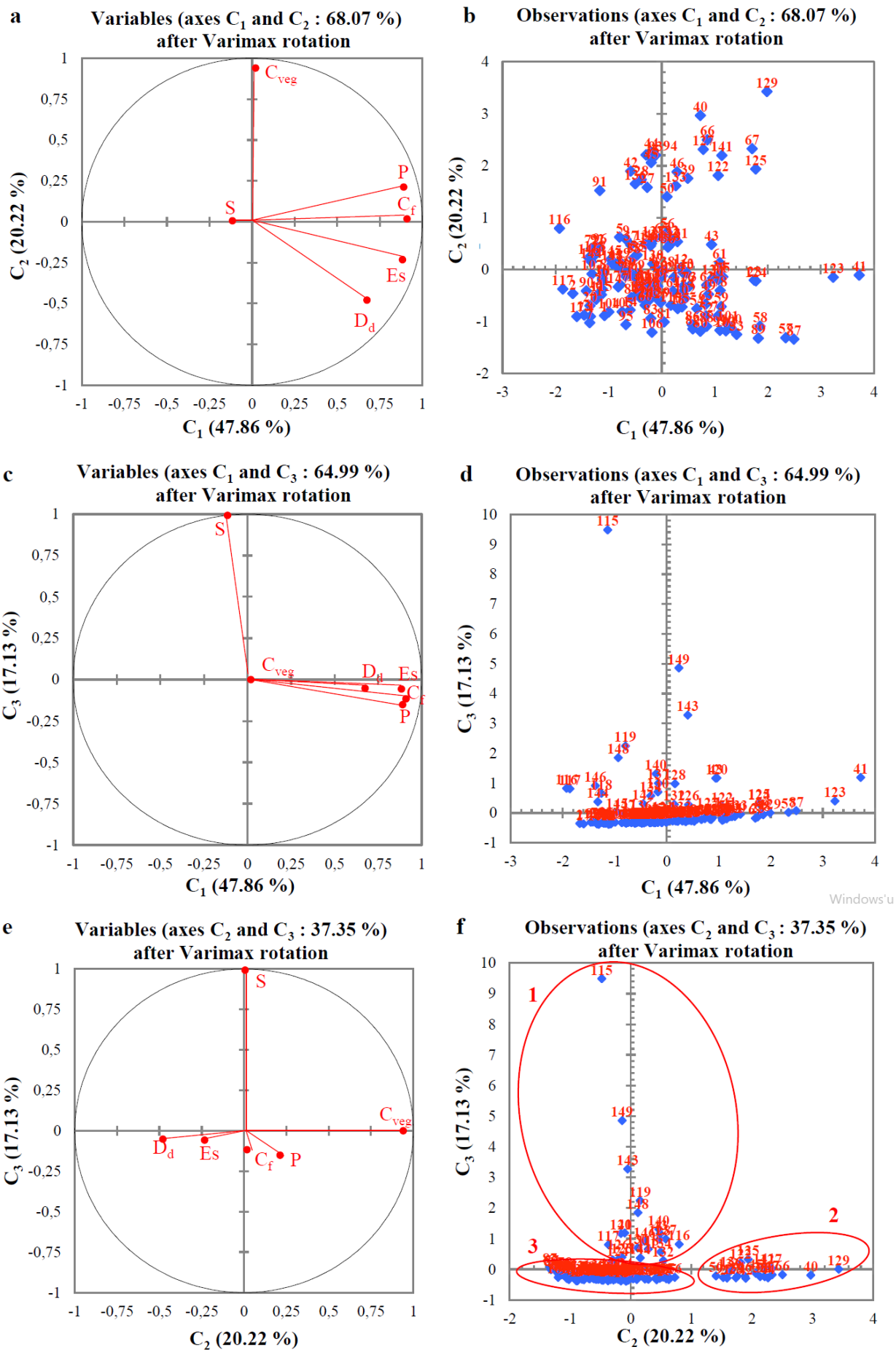

Figure 4. Correlation circles and projection of individuals on different axes

Table 2. Correlation matrix of multivariate analysis and regressive models (3rd group, 1st case).

Correlation matrix (1st case)						
Variables	Es	S	D_d	P	C_f	C_{veg}
Es	1					
S	-0.87	1				
D_d	0.66	-0.63	1			
P	0.84	-0.81	0.47	1		
C_f	0.82	-0.77	0.49	0.85	1	
C_{veg}	-0.53	0.58	-0.40	-0.35	-0.42	1
Regressive models (1st case)						
Variables	R^2	Models				
5 (S, D_d, P, C_f, C_{veg})	0.83	$Es = 2.85 \times S^{-0.132} \times D_d^{0.265} \times P^{0.493} \times C_f^{0.29} \times C_{veg}^{-0.037}$				
4 (S, D_d, P, C_f)	0.82	$Es = 3.23 \times S^{-0.16} \times D_d^{0.27} \times P^{0.164} \times C_f^{0.316}$				
3 (S, P, C_f)	0.80	$Es = 3.98 \times S^{-0.215} \times P^{0.362} \times C_f^{0.348}$				
2 (S, P)	0.79	$Es = 5.29 \times S^{-0.238} \times P^{0.661}$				
1 (S)	0.74	$Es = 41.35 \times S^{-0.368}$				

2nd Case: 3rd truncated group (100 values)

The correlation matrix (Table 3) shows clearly a general improvement of its corresponding coefficients. The obtained related models demonstrate that Es regression with five, four and three variables is constant in the sense that R^2 is too (R^2 = 0.97). The model with three variables is retained for nomograph development; it is formulated according to expression 3.

$$Es\ (T\ ha-1\ per\ year) = 16.68 \times S^{-0.375} \times P^{0.164} \times C_f^{0.204} \quad (3)$$

Table 3. Correlation matrix of multivariate analysis and regressive models (3rd group, 2nd case)

Correlation matrix (2nd case)						
Variables	Es	S	D_d	P	C_f	C_{veg}
Es	1					
S	-0.97	1				
D_d	0.66	-0.68	1			
P	0.88	-0.83	0.48	1		
C_f	0.86	-0.80	0.50	0.85	1	
C_{veg}	-0.55	0.57	-0.40	-0.32	-0.40	1
Regressive models (2nd case)						
Variables	R^2	Models				
5 (S, D_d, P, C_f, C_{veg})	0.97	$Es = 15.8 \times S^{-0.365} \times D_d^{0.015} \times P^{0.181} \times C_f^{0.191} \times C_{veg}^{-0.005}$				
4 (S, D_d, P, C_f)	0.97	$Es = 16.3 \times S^{-0.37} \times D_d^{0.014} \times P^{0.169} \times C_f^{0.193}$				
3 (S, P, C_f)	0.97	$Es = 16.68 \times S^{-0.375} \times P^{0.164} \times C_f^{0.204}$				
2 (S, P)	0.96	$Es = 21.1 \times S^{-0.394} \times P^{0.309}$				
1 (S)	0.95	$Es = 56.21 \times S^{-0.461}$				

Statistical analysis

The quality and reliability of the traced nomograph depend on the values of the calculated precision indices, it is often recommended to utilize a combination of these indices in order to obtain an accurate and complete evaluation of the numerical or graphic representation for quantifying water erosion. According to Isik (2013), Felegari et al. (2014) and Shirzadi et al. (2022), we chose the following indices: Mean Absolute Percentage Error (MAPE), Mean Square Deviation (MSD), Willmott Index (d), Coefficient of Determination (R^2) and the NASH criterion (NS), where each index contributed to decision-making regarding the validation and utilization of the developed graphical tool.

- MAPE is calculated according to the expression 4 based on deviations in absolute value between observations' measurements and those predicted compared to the measured values. It is expressed in %. A model representing perfectly the measured data will present a MAPE that is equal to 0.

$$MAPE = \sum_{i=1}^{N} \frac{\left|Es_{mes(i)} - Es_{pred(i)}\right|}{Es_{mes(i)}} \times \frac{100}{N};\ \left(MAPE \in [0, +\infty[\right) \quad (4)$$

With: Esmes represents the specific measured erosion; Espred is the specific predicted erosion by the nomograph and N is the observations' number.

- ASD, given by expression 5, is the value to be minimised for a prediction of values close to 0; the nomograph is considered as perfect.

$$ASD = \frac{\sum_{i=1}^{N}\left(Es_{pred(i)} - Es_{mes(i)}\right)^2}{N};\ \left(ASD \in [0, +\infty[\right) \quad (5)$$

- Index d, according to formula 6, measures the degree where predictions are exempt of errors. d varies between 0 and 1 where a value close to 1 indicates a perfect agreement between measured and predicted observations, while for a value close to 0, the prediction is in complete disagreement (Willmott, 1981).

$$d = 1 - \frac{\sum_{i=1}^{N}\left(P_i - O_i\right)^2}{\sum_{i=1}^{N}\left[\left|\left(P_i - \overline{O}\right)\right| + \left|\left(O_i - \overline{O}\right)\right|\right]^2};\left(0 \le d \le 1\right) \quad (6)$$

With: P(i) represents predicted values, O(i) and $\bar{O}$ are respectively values and average of measured observations.

- R2, determined by formula 7, measures prediction quality and ad adequacy between measured and predicted values by abacus, as it approaches to 1 and more abacus explains better the distribution of measured points.

$$R^2 = \frac{\sum_{i=1}^{N}\left(\left(Es_{pred(i)} - \overline{Es_{pred}}\right) \times \left(Es_{mes(i)} - \overline{Es_{mes}}\right)\right)}{\sqrt{\sum_{i=1}^{N}\left(Es_{pred(i)} - \overline{Es_{pred}}\right)^2} \times \sqrt{\sum_{i=1}^{N}\left(Es_{mes(i)} - \overline{Es_{mes}}\right)^2}};\left(0 \le R^2 \le 1\right) \quad (7)$$

- NS was defined in 1969 by Nash and improved in 1970 by Nash and Sutcliffe. It allows evaluating improvement brought by the used model compared to the reference model, generally average estimator. If Nash = 1, the abacus perfectly represents the data. When it is less than 0, this latter is a less-good estimator of measured data than their average, it is given by expression 8.

$$NS = 1 - \frac{\sum_{i=1}^{N}\left(Es_{mes(i)} - Es_{pred(i)}\right)^2}{\sum_{i=1}^{N}\left(Es_{mes(i)} - \overline{Es_{mes}}\right)^2};\left(NS \in]-\infty, 1]\right) \quad (8)$$

Results and Discussion

Nomograph elaboration

At the end of this work, a nomograph (or abacus) is established. The layout of this latter is based on abacus theory which corresponds to the graphic representation listed by mathematical laws defined by equations to any variable number (D'ocagne, 1899). Today, this discipline is designated under the name of "Nomography". It is natural to think that it is not possible in practice to nomograph with reasonable manner an equation of more than three variables while remaining in the two-dimensional plane (Pirio, 2010).

In our case, it is about an equation with four variables (Es, S, Cf and P) to be represented in a plane axis system. A transformation of equation (3) by separating it into two auxiliary functions easily nomografiable on the plan (Es1 and Es2 with three variables each) is indispensable, with:

$$Es_1 = f(S, C_f) = 4.084 \times S^{-0.375} \times C_f^{0.102} \quad (9)$$

$$Es_2 = f(P, C_f) = 4.084 \times P^{0.164} \times C_f^{0.102} \quad (10)$$

$$Es = Es_1 \times Es_2 \quad (11)$$

The developed nomograph is illustrated in Figure 5.

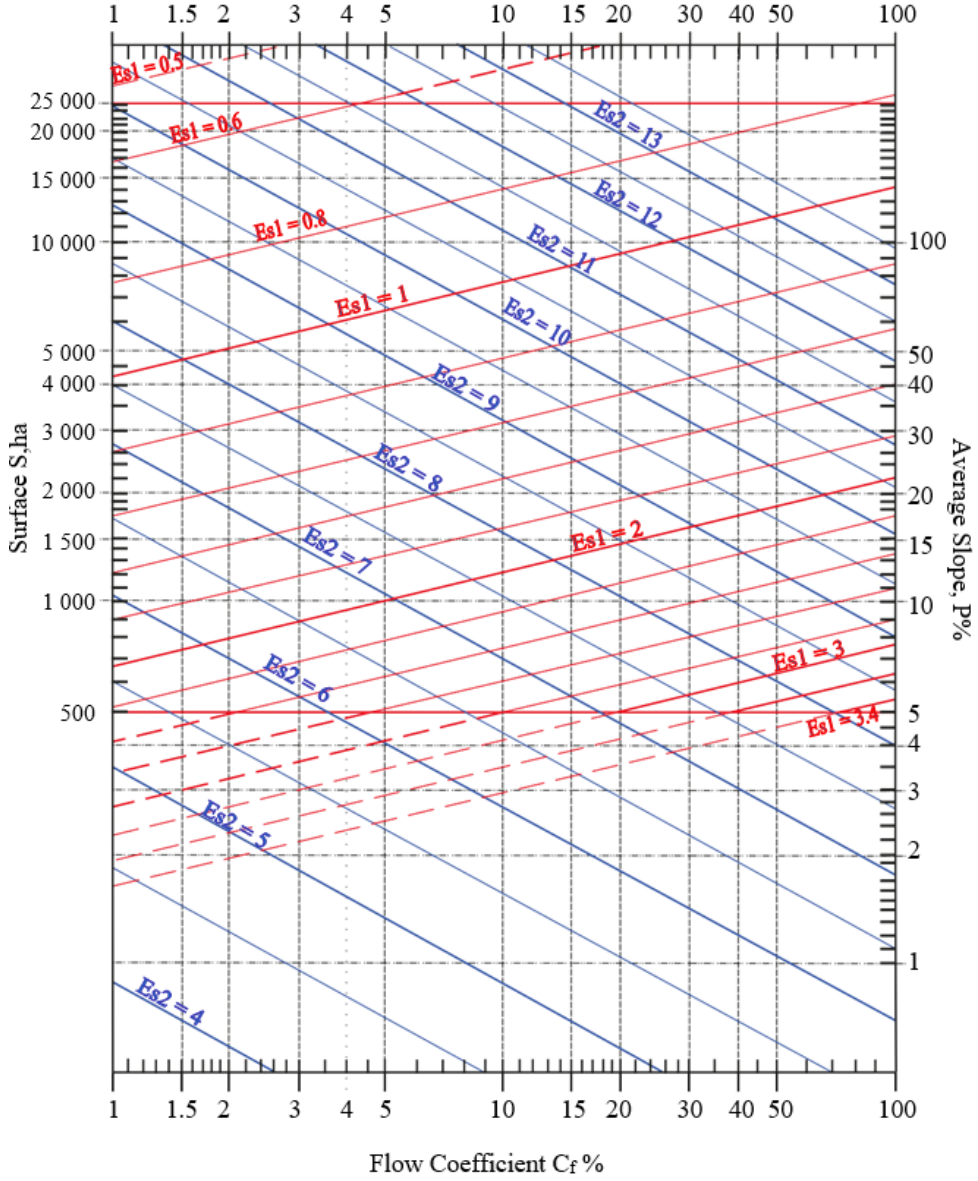

Figure 5. Nomograph of the specific erosion according to surface, average slope and flow coefficient for the Wadi Cheliff catchment

Nomograph validation

This validation step is a systematic process by which the reliability and accuracy of the developed nomograph was evaluated. Based on the 3rd group data resulting from the PCA for the plot, only 03 hydrometric stations and 97 hill dams out of a total of 20 and 114 structures were respectively selected, while all the 15 experimental sites of the dams were eliminated. Further, 20 sites of the remaining 100 were token as an example (Table 4) where we mentioned 03 different results, the 1st quantification of water erosion was based on experimental data, the second is performed since the multivariate analysis of the erosive action in relation to the involved factors, whereas the third was realized from the traced nomograph, which contributes to the determination of Es by knowing the Es1 and Es2 quantities calculated respectively by simple interpolation from the following couples of characteristics (S, Cf) and (P, Cf) of the corresponding catchment. However, this step must be accompanied by the calculation of the precision indices (Table 5) for a decision on the final result validation.

Table 4. Validation of Es (T ha^{-1} per year) results from nomographic quantification

Experimantal sites	Catchment caracteristics			Es_{exp}	Es_{ma}	$Es_{nmgrph} = Es_1 \times Es_2$		
	S (ha)	P (%)	C_f (%)			Es	E	Es_{nmgrph}
Hydrometric Station	16 300	13.12	21.52	7.34	6.83	0.82	8.39	6.88
	10 600	9.44	15.32	7.52	7.12	0.93	7.72	7.18
	12 550	11.39	17.06	7.53	7.04	0.89	8.00	7.12
Hill dams	20 540	6.81	5.02	4.64	4.24	0.65	6.50	4.23
	2 700	14.03	17.74	12.82	13.06	1.56	8.35	13.03
	2 585	12.66	16.05	13.09	12.80	1.60	8.06	12.90
	16 890	5.52	9.00	4.71	4.94	0.74	6.72	4.96
	632	17.88	22.26	23.73	24.47	2.70	8.96	24.19
	3 141	10.53	16.26	12.04	11.57	1.47	7.88	11.58
	1 166	13.26	16.61	17.89	17.50	2.17	8.18	17.75
	617	16.71	22.08	24.21	24.38	2.76	8.85	24.43
	24 980	6.55	9.70	4.05	4.45	0.65	6.90	4.46
	6 619	8.95	11.93	8.23	8.02	1.09	7.42	8.10
	4 453	10.95	13.58	9.52	9.87	1.27	7.77	9.87
	502	14.24	25.55	27.16	26.40	3.03	8.78	26.60
	21 150	5.85	8.68	4.79	4.55	0.68	6.73	4.58
	10 310	7.03	9.53	5.95	6.25	0.87	7.10	6.19
	767	13.81	19.55	21.12	21.27	2.53	8.38	21.23
	8 328	8.64	8.13	6.75	6.79	0.95	7.15	6.76
	4 787	10.48	15.66	9.40	9.80	1.25	7.82	9.78

Es_{exp}: Specific erosion from experimental data; Es_{ma}: Specific erosion from multivariate analysis; Es_{nmgrph}: Specific erosion from the developed nomograph.

The experimental results of specific erosion vary from 27.16 to 4.05 (T ha^{-1} per year) for respective areas from 502 to 24 980 ha, these same values were estimated by the nomograph at 26.60 and 4.46 (T ha^{-1} per year). On the one hand, we noted that all sites with catchment area > 25 000 ha were previously eliminated by the PCA, including some hydrometric stations and hill dams, but also all dams in the study area due to the impact of these structures on rivers and their downstream flow regimes (Assani et al., 2007; Yang et al., 2011). Thus, the influence of the watershed surface for the determination of the erosive action rate is decisive as well as the choice of sites because it plays a determining role in the regulation of precipitation concentration, the distribution of flows and therefore in the modulation of specific erosion. Moreover, because of elevated rates of sedimentation that do not adequately reflect actual quantities, places with catchment areas smaller than 500 ha were excluded. Therefore, the surface effect for our study was not significant regarding values between 500 and 25 000 ha in the Wadi Cheliff catchment.

In consideration of the precision indicators (Table 5) established for a 100 values samples distributed homogeneously over the entire study area, we found that the prediction of the values measured from the nomograph was very satisfactory. Furthermore, a low percentage of MAPE of 2% suggests that the graph estimated and the experimental values are matching and with more accuracy. Similarly, an excellent compatibility between the experimental observations and their predictions was indicated with values of R^2, d and NS equal to 0.99, which means that the nomograph has a remarkable ability to accurately reproduce observed or measured conditions by having an excellent fit to the field data and local conditions of the study area. This was confirmed by an ASD of 0.07 which indicated that absolute errors between nomographic predictions and their observations were relatively small, with limited dispersion.

Table 5. Accuracy index of specific erosion nomograph

Indexes	MAPE (%)	ASD	d	R^2	NS
Values	2	0.07	0.99	0.99	0.99

Conclusion

Due to the complexity of assessing water erosion rates at the catchment level especially the ungauged. The combination of a thorough analysis of hydrological, topographic and pedological factors with scientific and technological advances offers an integrated approach to estimate erosive risks and develop strategies for water and agricultural resource management.

Upon completion of our study, the findings indicate that the specific erosion varies annually from 4.46 to 26.60 T ha-1 on the catchment of Wadi Cheliff, classifying it as one of the Mediterranean rivers with the highest solid

inputs in the world relative to their average flow depth (Milliman, 2006). This magnitude is due to the fragility of the Mediterranean soils caused by irregular and often violent rainfall favoring erosion. In addition, significant slopes in many areas of hills and mountains exacerbate the phenomenon, while high temperatures accelerate the organic matter mineralization, as well as the often-reduced vegetation cover due to the climate and anthropogenic actions; therefore the soils are poorly protected (Plan Bleu, 2003; Özdemir, 2020).

Multivariate analysis allowed a regression model generation with nomographed functions, having as explanatory variables the surface, the flow coefficient and the average slope of the catchment with $R^2 = 0.99$. The nomograph was drawn according to the abacus theory, The product ($Es_1 \times Es_2$) provides the overall specific erosion values for the considered watershed, where each of the two quantities is obtained from the abacus by interpolation in function of the corresponding data. The tool is designed to be applied in the Wadi Cheliff catchment, for a Mediterranean climate with a semi-arid tendency and for areas between 500 and 25 000 ha which delineate the surface interval limits. Beyond this range, erosive action cannot be calculated due to the significant effect of the catchment area on specific erosion that takes into consideration the influence of rainfall distribution, topography, land use, soil type and management practices.

The nomograph is validated with a MAPE equal to 2%. Its reliability depends entirely on the availability of a credible, representative and precise database to ensure the validity of mathematical relationships and adjust its parameters to better adapt to the specific hydrological conditions of a given region. This graphic tool is recommended for its use simplicity, fast field estimation and decision support for territorial planning, which should be supported by identifying areas vulnerable to sediment production for appropriate treatment.

References

Abdellaoui, B., Merzouk, M., Aberkan, M., Albergel, J., 2002. Hydrological balance and siltation of the Saboun dam (Morocco). *Journal of Water Science* 5(4): 737-748.

Achite, M., Meddi, M., 2005. Spatial and temporal variability of streamflow and solid yields in semiarid areas. Case of the oued Mina basin (Northwest Algeria). *Journal of Water Science* 18: 37-56.

Ammari, A., 2012. Vulnérabilité à l'Envasement des Barrages (cas du bassin Hydrographique des Côtiers Algérois). PhD thesis. University of Biskra, Algeria. 195p. Available at [Access date: 18.09.2023]: http://thesis.univ-biskra.dz/id/eprint/68

Assani, A.A., Lajoie, F., Laliberté, C., 2007. The effects of dams on mean anual flow characteristics according to management mode and basin drainage area in Québec *Journal of Water Science* 20(1): 127-146.

Borges, A.L., 1993. Modélisation de l'érosion sur deux bassins versants expérimentaux des Alpes du Sud. PhD thesis. University of Grenoble I, France. 258p. Available at [Access date: 18.09.2023]: https://these.hal.science/tel-00764428

Bouanani, A., 2004. Hydrologie, transport solide et modélisation. Etude de quelques sous bassins de la Tafna (NW–Algérie). PhD thesis. University of Tlemcen, Algeria. 250p. Available at [Access date: 18.09.2023]: http://dspace1.univ-tlemcen.dz/handle/112/15094

Bouchelkia, H., Remini, B., 2003. Quantification du transport solide dans le bassin versant Algérien du Chellif. Ingénieries 33: 45-56. Available at [Access date : 18.09.2023]: https://hal-science/hal-00466014

Bouchnak, H., Felfoul, M.S., Boussema, M.R., Snane, M.H., 2009. Slope and rainfall effects on the volume of sediment yield by gully erosion in the Souar lithologic formation (Tunisia). *Catena* 78: 170-177.

D'ocagne, M., 1884. Procède Nouveau de calcul Graphique. Annales des Ponts et Chaussées 8, 531–540.

D'ocagne, M., 1899. Traité de la nomographie. Théorie des abaques, applications pratiques ; Gauthier-Villars, Paris. 496p.

Dagnelie, P., 1992. Statistique Théorique et Appliquée, Tome 1 – Les bases théoriques. Gembloux Agronomic Presses, vol 2, Belgique. 492p.

Dengiz, O., Demirkaya, S., 2022. Estimation and spatial distribution of some soil erodibility parameters in soils of Ilgaz Nationale Park. *Eurasian Journal of Soil Science* 11(1): 1-9.

Eisazadeh, L., Sokouti, R., Homaee, M., Pazira, E., 2012. Comparison of empirical models to estimate soil erosion and sediment yield in micro catchments. *Eurasian Journal of Soil Science* 1(1): 28-33.

El Kateb, H., Zhang, H., Zhang, P., Mosandl, R., 2013. Soil erosion and surface runoff on different vegetation covers and slope gradients: A field experiment in Southern Shaanxi Province, China. *Catena* 105: 1-10.

Elahcène, O., 2013. Etude du transport solide par charriage et en suspension dans le bassin versant de l'Oued Bellah (tipaza). PhD thesis. ENSA, El-Harrach, Algeria. 109 p.

Felegari, M., Talebi, A., Dastorani, M.T., Rangavar, A. S., 2014. Efficiency Assessment of Rangeland Hydrology and Erosion Model (RHEM) for water erosion quantification (Case study: Sangane Waterched-Iran). *Environmental Resources Research* 2(2): 134-146.

Heng, S., Suestugi, T., 2015. Regionalization of sediment rating curve for sediment yield prediction in ungauged catchments. *Hydrology Research* 46(1): 26-38.

Hotelling, H., 1933. Analysis of a complex of statistical variables into principal components. *Journal of Educational Psychology* 24: 417-441.

Isik, S., 2013. Regional rating curve models of suspended sediment transport for Turkey. *Earth Science Informatics* 6: 87–98.

Jahnke, H.N., 2012. Cauchy's Cours d'analyse. An Annotated Translation By Robert E. Bradley, and C. Edward Sandifer. Sources and Studies in the History of Mathematics and Physical Sciences. Dordrecht (Springer) 2009. *Historia Mathematica* 39: 460-479.

Kheniche, S., Louamri, A., Taabni, M., 2019. Estimation du transport solide et évolution de la relation "Débit liquid – debit solide" dans un basin semi-aride (Cas de l'oued Mellegue amont). *Algérie Orientale. Sciences & Technologie* D 50: 71-80.

Larfi, B., Remini, B., 2006. Le transport solide dans le bassin versant de l'Oued Isser. Impact sur l'envasement du barrage de Beni Amrane (Algérie). *Larhyss Journal* 5: 63-73.

Lee, S.E., Kang, S.H., 2014. Geographic information system-coupling sediment delivery distributed modeling based on observed data. *Water Science & Technology* 70(3): 495-501.

López-Tarazón, J.A., Batalla, R.J., Vericat, D., Balasch, J.C., 2010. Rainfall, runoff and sediment transport relations in a meso scale mountainous catchment: The River Isábena (Ebro basin). *Catena* 82: 23-34.

Meddi, M., Toumi, S., Assani, A.A., Eslamian, S., 2014. Regionalisation of rainfall erosivity in northern Algeria. *International Journal Hydrology Science and Technology* 4(2) :155-175.

Megnounif, A., Terfous, A., Ghenaim, A., Poulet, J.B., 2007. Key processes influencing erosion and sediment transport in a semi-arid Mediterranean area: the Upper Tafna catchment, Algeria. *Hydrological Sciences Journal* 52(6): 1271-1284.

Milliman, J.D., Sediment delivery from Mediterranean rivers: regional, global and temporal perspectives. Fluxes of small and medium-size Mediterranean rivers: Impact on coastal areas. In: Proceedings of the Mediterranean Science Commission, CIESM Workshop. 29 Mars-1 Avril 2006. Trogir, Croatia. pp. 67-71.

Mokhtari, E., 2005. Etude du transport solide par charriage dans l'Oued Mina et son impact sur l'envasement du barrage de Sidi M'hamed Ben Aouda (W, Relizane). Master's thesis. ENSH, Blida, Algeria. 95 p.

Najafova, N., 2022. System of measurs for soil erosion and protection. In: Proceedings of the International Soil Science Symposium on "Soil Science and Plant Nutrition". 2-3 December 2022. Samsun, Türkiye. pp. 195-198.

Ochoa, P.A., Fries, A., Mejía, D., Burneo, J.I., Ruíz-Sinoga, J.D., Cerdà, A., 2016. Effects of climate, land cover and topography on soil erosion risk in a semiarid basin of the Andes. *Catena* 140: 31–42.

Özdemir, N., 2020. Effects of land and plant managements on soil erodibility in the Turhal District of Tokat, Turkey. *Eurasian Journal of Soil Science* 9(4): 362-367.

Pirio, L., 2010. Géométrie anamorphique I : Abaques et Nomogrammes. Images des Mathématiques. CNRS, France. 21 p. Available at [Access date: 18.09.2023]: http://dml.mathdoc.fr/item/hal-00609226/

Plan Bleu, 2003. Les menaces sur les sols dans les pays méditerranéens. Etude bibliographique. Plan bleu pour la Méditerranée, Valbonne, France. 80p.

Remini, W., Remini, B., 2003. La sédimentation dans les barrages de l'Afrique du Nord. Courrier du Savoir 04: 65-69. Available at [Access date: 18.09.2023]: https://www.asjp.cerist.dz/en/article/77926

Rey, F., Ballais, J.L., Marre, A., Rovéra, G., 2004. Role of vegetation in protection against surface hydric erosion. *Comptes Rendus Géoscience* 336: 991–998.

Shen, H., Zheng, F., Wen, L., Han, Y., Hu, W., 2016. Impacts of rainfall intensity and slope gradient on rill erosion processes at loessial hillslope. *Soil and Tillage Research* 155: 429-436.

Shirzadi, A., Shahabi, H., Nabiollahi, K., Taghizadeh-Mehrjardi, R., Lizaga, I., Clague, J. J., Sushant, S. K., Golmohamadi, F., Ahmad, A., 2022. Towards robust smart data-driven soil erodibility index prediction under different scenarios. *Geocarta International* 37(26): 13176-13209.

Touaibia, B., 2000. Erosion- Transport solide- Envasement de barrage. Cas du bassin versant de l'Oued Mina (Wilaya de Relizane). PhD thesis, I.N.A. El Harrach, Algeria. 175p. Available at [Access date: 18.09.2023]: http://localhost:8080/xmlui/handle/123456789/2405

Touaibia, B., Achite, M., 2003. Contribution to the mapping of specific erosion in the Wadi Mina basin in the semiarid zone of northern Algeria. *Hydrological Sciences Journal* 48(2): 235-242.

Touaibia, B., Aidaoui, A., Gomer, D., Achite, M., 2001. Temporal quantification and variability of sediment discharge in a semiarid area in northern Algeria. *Hydrological Sciences Journal* 46(1): 41-53.

Tournès, D., 2000. NOTES & DEBATS pour une histoire du calcul graphique. Revue d'histoire des mathématiques 6 : 127-161. Available at [Access date : 18.09.2023]: http://www.numdam.org/item/RHM_2000__6_1_127_0

Tran Van, Q., 1961. Nomographie et statistique. Revue de statistique appliquée 9(3): 47-76. Available at [Access date: 18.09.2023]: http://www.numdam.org/item?id=RSA_1961__9_3_47_0

Willmott, C. J., 1981. On the validation of models. *Physical Geography* 2(2): 184-194.

Yang, S.L., Milliman, D.J., Li, P., Xu, K., 2011. 50,000 dams later: Erosion of the Yangtze River and its delta. *Global and Planetary Change* 75: 14-20.

Zhou, P., Luukkanen, O., Tokola, T., Nieminen, J., 2008. Effect of vegetation cover on soil erosion in a mountainous watershed. *Catena* 75: 319–325.